

Development of Pharmacophoric Models on 5,6-Diarylimidazo[2.1-b]thiazole for Selective Inhibition of Cyclooxygenase-2 Enzyme

R. SHARMA*, P. PRATHIPATI¹, S.C. CHATURVEDI² AND A. K. SAXENA¹

School of Pharmacy, Devi Ahilya Vishwavidyalaya, Takshshila Campus,
Khandwa Road, Indore-452017.

¹Division of Medicinal Chemistry, Central Drug Research Institute, Lucknow-226001.

²Department of Pharmacy, Shri Govindram Sakseria Institute of Technology and Science,
23, Park Road, Indore-452003.

Essential structural and physicochemical requirement in terms of common pharmacophoric sites and secondary sites for inhibitory action of 5,6-diarylimidazo(2.1-b)thiazole have developed by the molecular modeling studies using an APEX-3D expert system. In addition to this 3 dimensional quantitative structure activity relationship equations have also been developed. Among several pharmacophoric models three models (1,2,3) having $R^2 > 0.84$, chance < 0.04 , match > 0.80 , variables ≤ 3 with four pharmacophoric sites in two models (1 and 2) and three pharmacophoric sites in model no.3, one secondary site in model 1 and two secondary sites in model 2 and three secondary sites in model 3 describe the variation in selective inhibition of cyclooxygenase-2 enzyme. To validate our models we have attempted to predict the activity of prediction set compounds, Model 3 was found the best-fit model. Total hydrophobicity (global property), H-acceptor (presence) at one of the oxygen atom of sulphonyl methyl positively contributes for the inhibitory activity suggesting that total hydrophobicity and electrostatic interactions are favorable for selective inhibition of cyclooxygenase-2 enzyme.

Non-steroidal antiinflammatory drugs (NSAIDs) are widely used in the treatment of pain and inflammation. Most of them act through the inhibition of cyclooxygenase (COX) enzyme^{1,2}. Two isoenzymes of cyclooxygenase have been identified³: COX-1 and COX-2. The COX-1 being a constitutive enzyme is involved in different physiological process such as gastric cytoprotection, while COX-2 an inducible enzyme is expressed in the process of wide variety of inflammatory mediators. COX-2 appears to play a major role in the production of prostaglandin associated with inflammation response³⁻⁸. In view of that an ideal NSAIDs will be which inhibits COX-2 enzyme during the inflammation process, without modifying the physiological levels of constitutive enzyme COX-1^{9,10}. Most of the reported and

marketed selective COX-2 inhibitors belong to a tricyclic group of compounds with a central ring with the methyl sulphonyl or sulphonamide group at the para position of one of the aryl rings such as rofecoxib¹¹, and DuP-697¹². In view of that we have selected tricyclic 5,6-diarylimidazo [2.1-b]¹³ thiazole for quantitative structure activity relationship study to identify essential structural and physicochemical requirement in terms of common pharmacophoric sites and secondary sites.

MATERIALS AND METHODS

Selection of compounds and biological activity:

The compounds chosen for the present study were obtained from the literature¹³. The structure and biological activity values of the compounds forming the training set for all the molecules with definite IC_{50} values are shown in

*For correspondence

E-mail: rbsm73@yahoo.co.in

Table 1 and prediction set for the molecules with no definite IC_{50} values in table 2. The reported biological activity values for selective inhibition of COX-2 enzyme was converted into $-\log IC_{50}$.

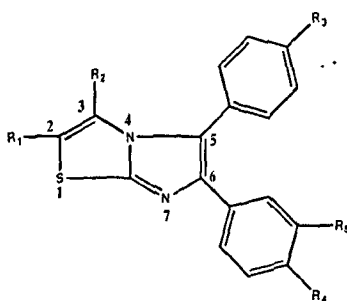
Workstation:

Molecular modeling and 3D QSAR studies were performed on a silicon graphics Indy R 4000 work station employing molecular simulations incorporations (MSI) software (Insight-II¹⁴ Discover¹⁵ and Apex-3D¹⁶).

Molecular 3D structure building, Energy minimization and Annealing:

3D molecular structures of all (eighteen) compounds were built in builder module of Insight II software. 3D structures were later fixed with angles and bond length by choosing fix button in the potential module; potential charge action, formal charge action and potential charge action were fixed. The structural energy minimization using CVFF forcefield¹⁷ was performed using the steepest descent, conjugate gradient, Newton Raphsons algorithms in

TABLE 1: INHIBITION OF COX-2 ENZYME BY 5,6-DIARYLIMIDAZO [2.1-B] THIAZOLE (TRAINING SET)



Compound	R ₁	R ₂	R ₃	R ₄	R ₅	COX-2 (IC ₅₀ μM)	COX-2 (- log IC ₅₀ μM)
01	H	H	4-MeSO ₂	H	H	0.016	1.7959
02	H	H	H	4-MeS	H	5.0	-0.6989
03	H	H	H	4-MeSO ₂	H	3.21	-0.5064
04	H	H	4-MeS	H	H	0.42	0.3767
05	Me	H	H	4-MeSO ₂	H	0.14	0.8539
06	H	H	4-MeSO ₂	F	H	0.014	1.8539
07	H	H	4-MeSO ₂	F	F	0.012	1.9208
08	Me	H	4-MeSO ₂	H	H	0.012	1.9208
09	H	Me	4-MeSO ₂	H	H	3.0	1.9100
10	Me	Me	4-MeSO ₂	H	H	5.0	-0.6989
11	H	Me	H	4-MeSO ₂	H	1.0	0.0000
12	H	CH ₂ CO ₂ Et	4-MeSO ₂	H	H	0.9	0.04575
13	Cl	H	4-MeSO ₂	Cl	H	0.016	1.7959
14	Cl	Cl	4-MeSO ₂	Cl	H	3.6	-0.5563

IC₅₀ values for the production of PGE2 in arachidonic acid stimulated Chinese hamster ovary cells transferred with human COX-2 enzyme.

TABLE 2: INHIBITION OF COX-2 ENZYME BY 5,6-DIARYLIMIDAZO [2.1-B] THIAZOLE (PREDICTION SET)

Compound	R ₁	R ₂	R ₃	R ₄	R ₅	COX-2 (IC ₅₀ M)	COX-2 (- log IC ₅₀ M)
01	Me	Me	H	4-MeSO ₂	H	> 5.0	> -0.6989
02	-CH=CH-CH=CH-		4-MeSO ₂	H	H	>5.0	> -0.6989
03	-CH=CH-CH=CH-		H	4-MeSO ₂	H	>5.0	> -0.6989
04	H	CH ₂ COOH	4-MeSO ₂	H	H	>5.0	> -0.6989

IC₅₀ values for the production of PGE2 in arachidonic acid stimulated Chinese hamster ovary cells transferred with human COX-2 enzyme.

sequence followed by quasi. Newton Raphson (Va09a)¹⁸ energy minimization techniques implemented in the discover module by using 0.001 kcal/mol. energy gradient convergence and maximum number of iteration set to 1000.

In order to check the validity of the above energy minimized techniques vis a vis other low energy conformations near global minimum, compound 7, which was one of the most active ones, was subjected to molecular dynamics (MD) simulations using CVFF force field¹⁹. In this procedure the atoms of the molecule were randomly assigned velocities based on the Maxwell-Boltzmann distribution and carrying out MD simulations at 1 fs at temp of T = 1000 K. The obtained average conformations of compound 7 by this calculation was used as starting point for another 5 ps of MD simulations at T=1000 K. The purpose of high temperature was to explore conformational space extensively. An Annealing procedure was subsequently applied to each average conformations obtained in high temperature simulations. The annealing was carried out as slow cooling down of the structure from 1000 to 300 K. The last step of an annealing procedure was energy minimization. Using this approach 20 conformations for a given starting geometry which gives a total of 75-150 ps of simulation time was obtained. The total energy of these 20 conformations ranged between 185.42 to 185.72 kcal. that was near to the conformational energy (185.4056 kcal.) obtained from the standard energy minimization procedure described above. Hence the same energy minimized conformations were used in the 3D-QSAR model development.

Automated identification of pharmacophore and 3D QSAR building:

The energy minimized structure were converted to MOPAC 6.0 version (MNDO Hamiltonian)¹⁹ for computational calculations of different physicochemical properties including: atomic charge, π -population, H-donor and

acceptor index, HOMO, LUMO, hydrophobicity, molar refractivity based on atomic contributions^{20,21}. The data was used by APEX-3D programme for automated identification of pharmacophore and 3D QSAR model building^{22,23}. The compounds with definite COX-2 inhibitory activity of 5,6-diarylimidazo[2.1-b]thiazole were classified into following classes (i). Very active (>1.7), (ii). Active (<1.7 and ≥ -0.60) (iii) Less active/inactive (>-0.60). The 3D QSAR equation were derived by defining COX-2 inhibitory activity ($-\log IC_{50}$) as a dependent variable and pharmacophoric center properties (π -population, charge, HOMO, LUMO, ACC_01, Don_01, hydrophobicity, refractivity), global properties (total hydrophobicity and total refractivity), secondary sites [H-acceptor (presence), H-donor presence), heteroatom (presence), hydrophobic (hydrophobicity), steric (refractivity)] and ring (presence) as independent variables with the occupancy set at 5, site radius at 0.80, sensitivity at 0.80 and randomization value at 100. Quality of each model was estimated from the R (coefficient of correlation), RMSA (calculated root mean square error based on all compounds with degree of freedom of correction), RMSP (root mean square error based on 'leave one out' with no degree of freedom correction), chance statistics and match parameter as detailed in our earlier paper²⁴.

RESULTS AND DISCUSSION

Among several 3D pharmacophoric models for all the molecules of training set two models, Model 1 and Model 2 were selected based on the criterion, correlation coefficient $R^2 > 0.8$, chance ≤ 0.01 , match value > 0.80 . These models described most accurately the distribution of the pharmacophores for the COX-2 inhibitory activity. (Table 3)

There were four pharmacophoric features in the two models, among them three pharmacophoric features were common in both the models, one site (A) being nitrogen at position four, second site (B) and third site (C) being sulfur

TABLE 3: 3D-QSAR MODELS DESCRIBING CORRELATION AND STATISTICAL RELIABILITY FOR COX-2 INHIBITORY ACTIVITY

Model	RMSA	RMSP	R ²	Chance	Size	Match	Variable	Compounds
01	0.44	0.46	0.85	0.000	4	0.82	1	14
02	0.39	0.41	0.89	0.010	4	0.81	2	14

RMSA: Calculated root mean square error based on all compounds with degree of freedom of correction, RMSP: Root mean square error based on 'leave one out' with no degree of freedom correction, R²: Square of correlation coefficient between experimental and approximated activity, Chance: Probability of chance correlation, Size: The number of pharmacophoric sites, Match: Quality of match for molecules having common pharmacophore, this varies from 0 to 1 with 1 meaning the best possible fit, Variable: The number of variable in the 3D QSAR model, Compounds: The number of compounds in the 3D QSAR model.

and its lone pair respectively at position one of 5,6-diarylimidazo [2.1-b] thiazole. The fourth pharmacophoric feature site (D) in Model 1 was a phenyl ring containing R₄ and R₅ substituents at para and meta positions attached at position six and in Model 2, this site corresponded to nitrogen at position seven. Three electron rich pharmacophoric sites A, B, C in both models are probably involved in electrostatic interactions while site D may involve in electrostatic interactions and hydrogen bonding in model 1 and 2, respectively.

The substrate-enzyme interactions in above two models for selective COX-2 inhibition not only depend on physicochemical properties of pharmacophoric centers corresponding to site A (π -population 0.616 \pm 0.002, charge hetero atom -0.099 \pm 0.002), site B (π -population 0.299 \pm 0.002, charge hetero atom 0.354 \pm 0.007, Don_01 6.259 \pm 0.001), site C (H-site1 \pm 0.000) and site D (cycle size 6.00 \pm 0.000, π electron 6.00 \pm 0.00) for Model 1 and site A (π -population 0.616 \pm 0.004, charge hetero atom -0.090 \pm 0.013), site B (π -population 0.302 \pm 0.011, charge hetero atom 0.356 \pm 0.024, Don_01 6.265 \pm 0.0502), site C (H-site 1.00 \pm 0.000) and site D (π -population 1.013 \pm 0.003, charge hetero atom -0.1532 \pm 0.006, Don_01 8.832 \pm 0.062)^a, for Model 2 but also on their spatial disposition; the mean inter atomic distances of four pharmacophoric sites A,B,C,D are A-B (2.594 \pm 0.0026), A-C (5.532 \pm 0.0021), A-D (5.139 \pm 0.0020), B-C (2.995 \pm 0.0010), B-D (6.352 \pm 0.0083), C-D (8.171 \pm 0.005) Å for Model 1 (fig. 2) and A-B (2.595 \pm 0.003), A-C (5.534 \pm 0.002), A-D (2.371 \pm 0.006), B-C (2.995 \pm 0.005), B-D (2.690 \pm 0.001), C-D (4.724 \pm 0.004) and Å for Model 2. (fig. 3)

In order to understand the interaction and to identify the important pharmacophore and secondary sites for explaining the variation in COX-2 inhibitory activity data, 3D

QSAR equations were also derived using these pharmacophores as a template for superimposition. COX-2 inhibitory activity was correlated with H-acceptor (presence)

TABLE 4: PARAMETER VALUES FOR SECONDARY SITES IN MODEL 1 AND MODEL 2

Compound	Model 1 ^d	Model 2 ^d	
	H-acceptor (Presence) at site SS1x	H-acceptor (Presence) at site SS2x	H-acceptor (Presence) at site SS2y
01	1.000	1.000	1.000
02	—	—	—
03	—	—	—
04	—	—	—
05	—	—	—
06	1.000	1.000	1.000
07	1.000	1.000	1.000
08	1.000	1.000	1.000
09	—	—	1.000
10	—	—	1.000
11	—	—	—
12	—	—	—
13	1.000	1.000	1.000
14	—	—	1.000

^d(---) indicates absence of property. Secondary site H-acceptor (presence) at SS1x for model 1 and SS2x and SS2y for model 2. (Fig. 1)

at secondary site, SS1x (7.416 ± 0.005 , 9.942 ± 0.008 , 12.924 ± 0.005 and 8.774 ± 0.018 Å from the pharmacophoric sites A, B, C and D, respectively) in the Model 1 (Eqn. 1) and site SS2x (7.414 ± 0.005 , 9.943 ± 0.008 , 12.924 ± 0.005 , 9.084 ± 0.005 from the pharmacophoric sites A, B, C and D, respectively) in Model 2 (Eqn. 2) at one of the oxygen of sulphonyl methyl group and H-acceptor (presence) at secondary site SS2y (fig. 1) at second oxygen atom of the sulphonyl methyl group (7.160 ± 0.042 , 10.195 ± 0.035 , 13.046 ± 0.006 , 8.796 ± 0.005 Å from the pharmacophoric sites A, B, C and D, respectively) in the Model 2. The common secondary site SS1x in Model 1 and SS2x in Model 2 positively contribute for activity probably involved in hydrogen bonding with COX-2 enzyme. The other secondary site SS2y in Model 2 negatively contributes for activity suggesting that this hydrogen-bonding site is not favorable for inhibitory

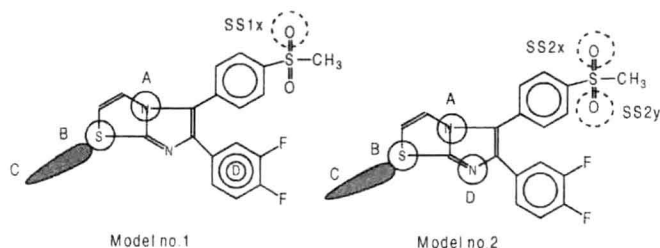


Fig. 1: Pictorial Representation of Pharmacophoric \bigcirc and Secondary \bigcirc sites represented on one of the most active compound 7.

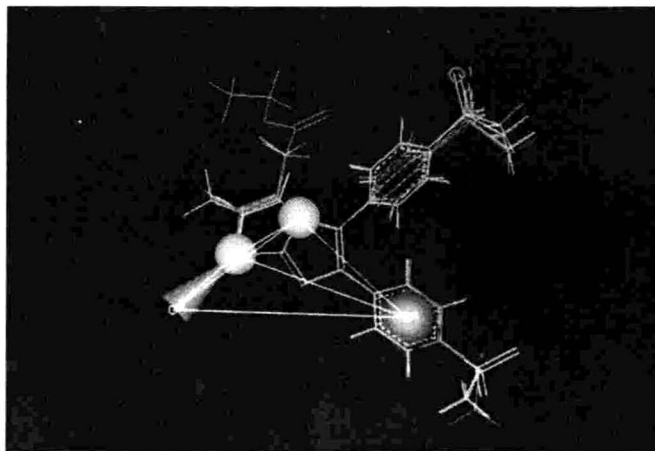


Fig. 2: Superimposition of the compounds 1-14 with pharmacophore sites in Model 1.

Superimposition of the compounds 1-14 (training set) with pharmacophore sites (solid spheres) and secondary sites (circle); a pharmacophoric pattern for selective COX-2 inhibition in Model 1.

activity. The Eqn. 1 and 2 show a good correlation coefficient values, $R = 0.922$ and 0.946 of high statistical significance $>99\%$. ($F_{1,12} \alpha_{0.001} = 22.2$; $F_{1,12} = 68.4$ and $F_{2,11} \alpha_{0.001} = 16.4$; $F_{2,11} = 46.8$ for Model 1 and Model 2, respectively).

$$-\log IC_{50} = 2.042(\pm 0.247)[H_{Acc} \text{ at SS1x}]^b - 0.185, n=14, R=0.922, R^2=0.851, F_{1,12}=68.4 \dots \text{Eqn.1.}$$

$$-\log IC_{50} = 2.435(\pm 0.284)[H_{Acc} \text{ at SS2x}]^b - 0.589 (\pm 0.275) [H_{Acc} \text{ at SS2y}]^b + 0.012, n = 14, R=0.946, R^2=0.895, F_{2,11}=46.8 \dots \text{Eqn.2, } ^b (H_{Acc} - \text{H-acceptor})$$

Both these models with good superimposition (figs. 2 and 3) for all compounds (Match Value >0.80) and with good predictive power as evidenced by low chance values (0.000 and 0.010 for Model 1 and Model 2, respectively) with almost similar RMSA and RMSP values explained the observed activity data in most of the cases but did not predict less active compound ($IC_{50} > 5$) of test set. Hence knowing that 3 parameter equation with fourteen compounds is not well accepted conventionally, the best such model (Model 3) was studied and used for predicting the activity of test set compounds.

This model had three pharmacophoric sites corresponding to site A (π -population 1.013 ± 0.001 , charge hetero atom -0.153 ± 0.002 , Don_01 8.832 ± 0.017), site B (π -population 0.302 ± 0.003 , charge hetero atom 0.356 ± 0.007 , Don_01 6.265 ± 0.013), site C (H-site 1.000 ± 0.000) and

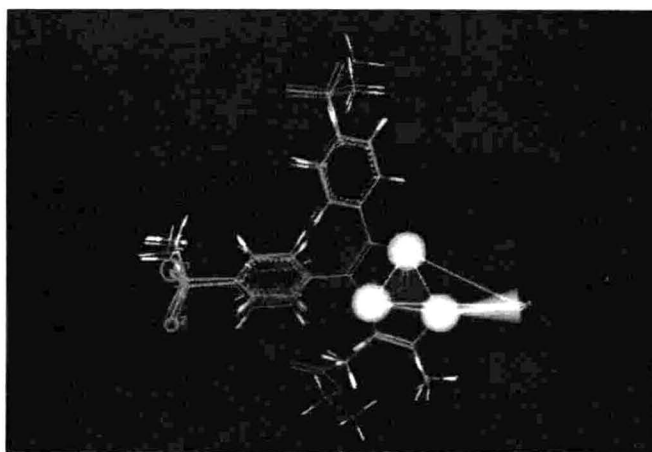


Fig. 3: Superimposition of the compounds 1-14 with pharmacophore sites in Model 2.

Superimposition of the compounds 1-14 (training set) with pharmacophore sites (solid spheres) and secondary sites (circle); a pharmacophoric pattern for selective COX-2 inhibition in Model 2.

spatial arrangements [A-B (2.690 ± 0.001), A-C (4.724 ± 0.004), B-C (3.000 ± 0.000)], secondary sites (SS3x; H-acceptor ;presence [9.082 ± 0.003 , 9.950 ± 0.009 , 12.933 ± 0.010 Å from pharmacophoric sites A, B and C, respectively] at one of oxygen atom of sulphonyl methyl and SS3y refractivity [4.914 ± 0.042 , 4.072 ± 0.047 , 6.936 ± 0.047 Å from pharmacophoric sites A, B and C, respectively] at R_2 substitution) and global property; total hydrophobicity showed good correlation coefficient $R=0.933$ of high statistical significance $>99\%$. ($F_{3,10} \alpha_{=0.001}=15.00$; $F_{3,10}=22.58$) with good predictive power (chance value; 0.03) and superimposition (match value; 0.81) and explained the selective COX-2 inhibition of not only in the training set but two test compounds (2 and 3) perfectly well and other two compounds (1 and 4) relatively better than Model 1 and 2.

The Model 3 (Eqn. 3) was also similar to Model 1 and Model 2 both in terms of the three pharmacophoric sites A, B and C with spatial arrangements and also for one secondary site H-acceptor site SS3x at one of the oxygen

atom of sulphonyl methyl group. It differed only in other secondary site SS3y in terms of refractivity at R_2 substitution, and global property; total hydrophobicity.

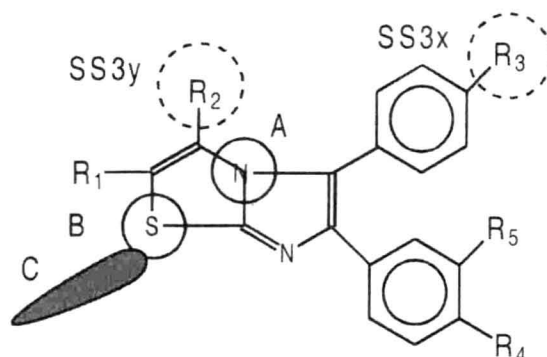


Fig. 4: Pictorial Representation of Pharmacophoric \bigcirc and Secondary \bigcirc sites presented in Model 3.

TABLE 5: EXPERIMENTAL, CALCULATED AND PREDICTED ACTIVITY DATA ($-\log IC_{50} \mu M$) FOR COX-2 INHIBITORY ACTIVITY IN MODEL 1 AND MODEL 2

Compound	Experimental	Model 1		Model 2	
		Calculated	Predicted	Calculated	Predicted
01	1.80	1.86	1.87	1.80	1.87
02	-0.70	-0.18	-0.12	-0.70	0.15
03	-0.51	-0.81	-0.14	-0.51	0.12
04	0.38	-0.18	-0.25	0.38	-0.06
05	0.85	-0.18	-0.31	0.85	-0.16
06	1.85	1.86	1.86	1.85	1.86
07	1.92	1.86	1.84	1.92	1.84
08	1.92	1.86	1.84	1.92	1.84
09	-0.48	-0.18	-0.15	-0.48	-0.63
10	-0.70	-0.18	-0.12	-0.70	-0.52
11	0.00	-0.18	-0.21	0.00	0.01
12	0.05	-0.18	-0.21	0.05	0.01
13	1.80	1.86	1.87	1.80	1.87
14	-0.56	-0.18	-0.14	-0.56	-0.59

Experimental: Experimental activity data in the form of $-\log IC_{50} \mu M$, Calculated: Activity values calculated according to the 3D QSAR model, Predicted: Activity values predicted using cross validation.

TABLE 6: 3D-QSAR MODELS DESCRIBING CORRELATION AND STATISTICAL RELIABILITY FOR COX-2 INHIBITORY ACTIVITY OF MODEL 3

Model	RMSA	RMSP	R ²	Chance	Size	Match	Variable	Compounds
03	0.48	0.58	0.87	0.030	3	0.81	3	14

RMSA: Calculated root mean square error based on all compounds with degree of freedom of correction, RMSP: Root mean square error based on 'leave one out' with no degree of freedom correction, R²: Square of correlation coefficient between experimental and approximated activity, Chance: Probability of chance correlation, Size: The number of pharmacophoric sites, Match: Quality of match for molecules having common pharmacophore, this varies from 0 to 1 with 1 meaning the best possible fit, Variable: The number of variable in the 3D QSAR model, Compounds: The number of compounds in the 3D QSAR model.

$-\log IC_{50} = -0.371(\pm 0.170)TH^c + 1.704(\pm 0.268)H_{acc}^c(\text{presence}) \text{ at site SS3x} - 0.269(\pm 0.065)Ref^c \text{ at site SS3y} + 1.603b$. Eqn.3

$n=14$, $r=0.933$, $r^2=0.870$, $F_{1,12}=22.58$, $^c(TH\text{-total hydrophobicity}, H_{acc}\text{-H-acceptor}, Ref\text{-Refractivity})$

In conclusion, 5,6-diaryl imidazo[2.1-b]thiazole was used in the present study to determine essential structural and physicochemical properties in terms of common pharmacophoric features for selective COX-2 inhibitory activity. The generated pharmacophores were used as a template for development of 3D QSAR models. A comparison of the more robust pharmacophoric Model 3 as compared to Model 1 and 2 suggested that three

pharmacophoric features one on nitrogen at position four, two and three on sulfur and its lone pair at position one common to all three models were almost same in terms of physicochemical properties (π -population, charge

TABLE 7: PARAMETER VALUE FOR SECONDARY SITES IN MODEL 3

Compound	Model 3 ^a		
	Total Hydrophobicity	H-acceptor at site SS3x	Refractivity at site SS3y
01	3.750	1.000	—
02	4.700	—	—
03	3.750	—	—
04	4.700	—	—
05	3.300	—	—
06	3.900	1.000	—
07	4.000	—	—
08	3.300	1.000	—
09	3.300	—	2.950
10	2.850	—	2.950
11	3.300	—	2.950
12	3.150	—	2.900
13	4.950	1.000	—
14	5.600	1.000	6.150

^a(---) indicates absence of property, Global property; total hydrophobicity and secondary sites H-acceptor (presence) at SS3x and Refractivity at SS3y. (Fig. 4)

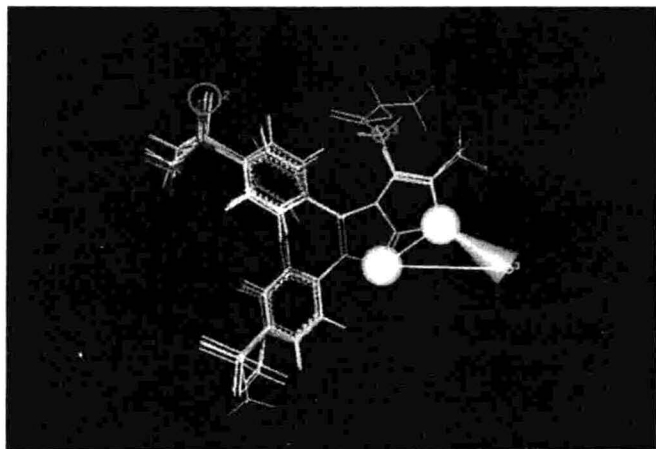


Fig. 5: Superimposition of the compounds 1-14 with pharmacophore sites in Model 3.

Superimposition of the compounds 1-14 (training set) with pharmacophore sites (solid spheres) and secondary sites (circle); a pharmacophoric pattern for selective COX-2 inhibition in Model 3.

TABLE 8: EXPERIMENTAL, CALCULATED AND PREDICTED ACTIVITY DATA (- LOG IC₅₀ μM) FOR COX-2 INHIBITORY ACTIVITY IN MODEL 3

Compound	Experimental	Calculated	Predicted
01	1.80	1.92	1.95
02	-0.70	-0.14	0.17
03	-0.51	0.21	0.36
04	0.38	-0.14	-0.43
05	0.85	0.38	0.28
06	1.85	1.86	1.86
07	1.92	1.82	1.80
08	1.92	2.08	2.15
09	-0.48	-0.41	-0.40
10	-0.70	-0.25	-0.07
11	0.00	-0.41	-0.51
12	0.05	-0.34	-0.45
13	1.80	1.47	1.35
14	-0.56	-0.42	0.48

Experimental: Experimental activity data in the form of -log IC₅₀ μM, Calculated: Activity values calculated according to the 3D QSAR model, Predicted: Activity values predicted using cross validation.

heteroatom, Don_01 and H-site) and spatial disposition for specific interaction with COX-2 enzyme well explained the activity of test set. These pharmacophoric centers may be involved in binding to an adjacent pocket to cyclooxygenase active site and the aryl ring with R₄ and R₅ substitution is probably involved in a hydrophobic cavity of COX-2 enzyme. Among the secondary sites one common site in all three models corresponding to H-acceptor (presence) on one of the oxygen atom of sulphonyl methyl is favorable for selective COX-2 inhibition and likely involved in hydrogen bonding with one of the amino acid in the active site of COX-2 enzyme. This study thus brings important structural insight to aid design of novel selective COX-2 inhibitors by judicious structural modulation.

ACKNOWLEDGEMENTS

The authors are thankful to Director, CDRI, Lucknow for his interest, to Mr. A. S. Kushwaha for the technical assistance and two of us (RS and PP) are grateful to CSIR,

TABLE 9: EXPERIMENTAL AND PREDICTED BIOLOGICAL ACTIVITY BY DIFFERENT PHARMACOPHORIC MODELS FOR THE COMPOUNDS OF PREDICTION SET

Compound	Experimental	Predicted		
		Model 1	Model 2	Model 3
01	> -0.6989	-0.18	0.01	-0.25
02	> -0.6989	-0.18	-0.58	-1.18
03	> -0.6989	-0.18	0.01	-1.18
04	> -0.6989	-0.18	0.01	-0.21

Experimental: Experimental activity data in the form of -log IC₅₀ μM, Predicted: Activity values predicted using cross validation.

New Delhi for Research fellowships and RS is thankful to Dr. S. Bharti, Head, School of Pharmacy and Rector, D. A. V. V. Indore for his interest.

REFERENCES

- Vane, J.R., *Nature*, 231, 1971, 232.
- Lombardino, J.G., In; *Nonsteroidal Anti-inflammatory Drugs*; Wiley-Interscience / John Wiley & Sons, New York, 1985, 255.
- Fu, J.Y., Masferrer, J.L., Seibert, K., Raz, A. and Needleman P., *J. Biol. Chem.*, 265, 1990, 16737.
- Seibert, K., Zhang, Y., Leahy, K., Hauser, S., Masferrer, J. and Isakson, P., *Adv. Exp. Med. Biol.*, 400A, 1997, 167.
- Kujubu, D.A., Fletcher, B.S., Varnum, B.C., Lim, R.W. and Herschman, H.R., *J. Biol. Chem.*, 266, 1991, 12866.
- Lee, S.H., Soyoola, E., Chanmugan, P., Hart, S., Sun, W., Zhong, S., Licu, D., Simmons, D. and Hwang, D., *J. Biol. Chem.*, 267, 1992, 25934.
- O'sullivan, M.G., Huggins, E.M. Jr. and Mc Call, C.E., *Biochem. Biophys. Res. Commun.*, 191, 1993, 1294.
- Dannhardt, G. and Kiefer, W., *Eur. J. Med. Chem.*, 36, 2001, 109.
- Reitz, D.B. and Seibert, K., *Ann. Rep. Med. Chem.*, 30, 1995, 179.
- Pairet, M., Churchill, W., Roman, R.J., Haber, S.B., Kerr, J.S., Schmidt, W.K., Smith, C., Hewes W.E. and Ackerman, N.R., *J. Pharmacol. Exp. Ther.*, 254, 1990, 180.
- Desmond, R., Dolling, U., Marcune, B., Tillyer, R. and Tschaen D., *World Patent No. WO96/08482*, 1996, Through *Chem. Abstr.*, 1996, 125, 86474.
- Gans, K.R., Galbraith, W., Roman, R.J., Haber, S.B., Kerr, J., Schmidt, S., Smith C., Hewas, E. and Ackerman N.R., *J. Pharmacol. Exp. Ther.*, 1990, 254, 180.
- Therien, M., Brideau, C., Chan, C.C., Cromlish, W.A., Gauthier, J.Y., Gordon, R., Greig, G., Kargman, S., Lau, C.K., Leblanc, Y., Li, C-S., O'Neill, G.P., Riendeau, D., Roy, P., Wang, Z., Xu, L. and Prasit, P., *Bioorg. Med. Chem. Letters*, 1997, 7, 47.

14. Apex-3D version 1.4 user guide, Biosym MSI, San Diego, Sept. 1993.
 15. Insight II version 2.3.0, Biosym MSI, San Diego, Sept. 1993.
 16. Discover version 3.1 user guide, Biosym MSI, San Diego, Sept. 1993.
 17. Dabur-ostguthorpe, P., Roberts, V.A., Ostguthorpe, D.J., Wolf, J., Genset, M. and Hagler, A.T., **Proteins Struct. Func. Genet.**, 1988, 4, 31.
 18. Powell, M.J.D. **Math. Program.**, 197, 241.
 19. Stewart, J.J.P., **QCPF Bull.**, 1990, 455.
 20. Ghose, A.K. and Crippen, G.M., **J. Chem. Inf. Comput. Sci.**, 1987, 27, 21.
 21. Viswanadhan, V.N., Ghose, A.K., Revankar, G.R. and Robins, R.K., **J. Chem. Inf. Comput. Sci.**, 1989, 29, 103.
 22. Golender, V.E. and Vorpapel, E.R., In; Kubinyi, H., Eds., **3D QSAR in Drug Design Theory, Methods and Application**, Escom, Leiden, 1993, 137.
 23. Golender, V.E. and Rozenblit, A.B., In; **Logical and Combinatorial Algorithms Drug Design**, Research Studies Press, Letchworth, 1983, 1.
 24. Pandya, T., Pandey, S.K., Tiwari, M., Chaturvedi, S.C. and Saxena, A.K., **Bioorg. Med. Chem.**, 2001, 9, 291.
-